THE JOURNAL OF PHYSICAL CHEMISTRY B

Article

pubs.acs.org/JPCB

Supramolecular "Leeks" of a Fluorinated Hybrid Amphiphile That Self-Assembles into a Disordered Columnar Phase

Mohan N. Wadekar,[†] Ludmila Abezgaus,[⊥] Kristina Djanashvili,[§] Wolter F. Jager,*[,‡] Eduardo Mendes,[†] Stephen J. Picken,*[,†] and Danino Dganit[⊥]

[†]NanoStructured Materials and [‡]Nano-Organic Chemistry, Department of Chemical Engineering, and [§]Biocatalysis and Organic Chemistry, Department of Biotechnology, Delft University of Technology, Julianalaan 136, 2628BL Delft, The Netherlands

[⊥]Department of Biotechnology and Food Engineering and the Russell Berrie Nanotechnology Institute, Technion−Israel Institute of Technology, Haifa 32000, Israel

Supporting Information

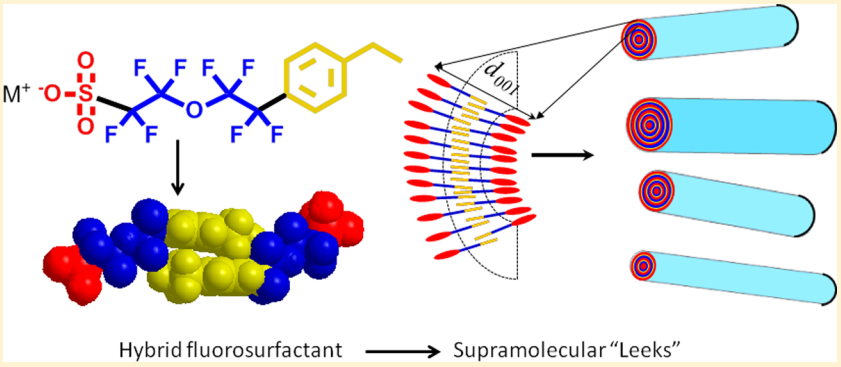

ABSTRACT: We report on the formation of unprecedented "leek"-shaped aggregates of an anionic fluoroalkyl sulfonate surfactant (**FS**) and the supramolecular assembly of these aggregates into a disordered columnar phase (C_S). The leeks are formed by wrapping of 2−4 **FS**−water bilayers of thickness 26−28 Å into 10−20 nm thick and >100 nm long structures, in the concentration regime of 63−70 wt % **FS**. A lamellar (L_α) lyotropic liquid-crystalline (LLC) phase forms at higher concentration, between 70 and 84 wt %. In the two LLC phases, the **FS** molecules were organized in an interdigitated or tilted fashion, or a combination of the two. Such a unique supramolecular self-assembly of amphiphiles has not been predicted nor observed before. This self-assembly behavior could be of interest to various fields like microencapsulation, nanomedicine, and membrane protein crystallization.

1. INTRODUCTION

Amphiphilic molecules like surfactants and lipids are well-known to form micellar and lyotropic liquid-crystalline (LLC) mesophases in strongly polar solvents like water. In general, LLC phase behavior is controlled by the hydrophobicity of amphiphiles, their packing characteristics, which are defined by the architecture, and global packing constraints imposed by the volume fraction.[1] The packing characteristics are described in terms of the local curvature at the hydrophobic−hydrophilic layer interface, which is expressed in terms of the critical packing parameter (CPP).[1,2]

Fluorinated surfactants are amphiphiles with fluorine instead of hydrogen atoms attached to the hydrophobic tail. Insertion of strongly electronegative fluorine atoms considerably affects their physical and chemical properties. For example, fluorinated surfactants are thermally and chemically more stable than hydrocarbon surfactants. Because fluorine atoms are bigger than hydrogen atoms, fluorinated surfactants are bulkier and stiffer compared to hydrogenated ones. This fact induces all-trans conformations in fully fluorinated tails.[3] Thus, fluorinated surfactants display quite different packing behavior from their hydrogenated counterparts.[4] Furthermore, fluorocarbons display weak van der Waals interactions that lead to weaker intermolecular cohesive forces and enhanced hydrophobicity compared to the hydrogenated analogues.[2,5,6] Because of these reasons, the physical properties of fluorinated surfactants, like phase behavior, lyotropic LC phase morphology, and rheology, are drastically modified.[2]

The LLC phase behavior of fluorinated surfactants and hybrid surfactants with fluorocarbon and hydrocarbon tails has not been studied as extensively as that of hydrocarbon-based surfactants. From a fundament point of view, it is interesting to study the differences in phase behavior between fluorinated and hydrogenated surfactants with similar molecular structures and to investigate the effect of a fluorinated structure in the hydrophobic tail on the LLC phase behavior and morphology.

Received: November 16, 2012
Revised: February 10, 2013
Published: February 11, 2013

dx.doi.org/10.1021/jp311337z | J. Phys. Chem. B 2013, 117, 2820−2826

The LLC phase behavior of ionic[2,7−10] and nonionic[11,12] fluorinated surfactants and hybrid fluorocarbon−hydrocarbon surfactants[13−15] has been investigated in the past. Tetraalkyl ammonium as well as inorganic metal salts of perfluorinated carboxylic acids have been studied in detail,[7] and generally, phase diagrams of these compounds exhibit lamellar (L_α), normal hexagonal (H_1), and reverse hexagonal (H_2) mesophases. An additional complex hexagonal (H_C) phase in the binary lithium perfluorooctanoate−water system[9] has been reported by Tiddy and co-workers. This phase was made of surfactant bilayers arranged into hollow pipes that assembled in hexagonal symmetry. For the tetramethyl ammonium perfluorodecanoate−water system,[3] a novel rhombohedral intermediate mesh (Mh_1) phase[16] was reported by Holmes and co-workers. Similarly, cubic bicontinuous (V) mesophases, which are rarely found in hydrogenated systems,[10] have been reported for sodium and ammonium salts of homologous perfluoroether carboxylic acid surfactants.

The phase behavior of fluoroalkyl sulfonate surfactants is not extensively reported upon, which may be caused by their poor solubility in water at ambient temperature.[17] One of the few explored systems is lithium perfluorooctane sulfonate (LiFOS)−water.[18] This system exhibits lamellar (L_α), hexagonal (H_1), and bicontinuous (V) phases and a phase diagram that is qualitatively similar to that of lithium dodecyl sulfate (LiDS).

Hybrid surfactants containing a hydrophilic, a hydrocarbon, and a fluorocarbon segment generally exhibit a more complex phase behavior. This is due to the fact that the three phases have a tendency to phase separate. Surfactant systems like the star polyphile, reported by Hyde et al.,[14] display a tilted hexagonal phase, in which the fluorocarbon and hydrocarbon chains are phase-separated within the hydrophobic domains. Interestingly, a hybrid phospholipid[19] and a zwitterionic hybrid surfactant[20] have been reported to form nano- and microtubules by wrapping up of 2−3 bilayers. However, these multilayer assemblies are formed at low concentrations, 3 and 6 wt %, respectively.[21]

Here, we report on the phase behavior of sodium 1,1,2,2-tetrafluoro-2-(1,1,2,2-tetrafluoro-2-(4-ethylphenyl)ethoxy)-ethanesulfonate (**FS**) (Figure 1), a sulfonated hybrid fluorosurfactant designed in our laboratory.[22] This compound has an unusual topology, with the sulfonate head group attached to a short perfluoroether group, which is attached to an ethylbenzene moiety at the other side. **FS** is highly water-soluble at room temperature and forms an unprecedented columnar LLC phase composed of "leek"-like supramolecular aggregates, which are composed of multiple **FS** bilayers. To the best of our knowledge, this is the first supramolecular LLC phase composed of multilamellar anisotropic entities. Apart from this supramolecular phase, composed of multiwalled leeks, we have also identified a conventional lamellar (L_α) phase at higher surfactant concentrations. The phase behavior of **FS** in water has been investigated using optical polarized light microscopy (OPM), small-angle X-ray scattering (SAXS), ^{2}H NMR, and freeze-fracture transmission electron microscopy (FF-TEM).

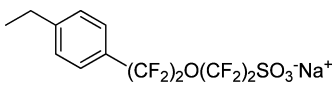

FS

Figure 1. Molecular structures of **FS**.

2. EXPERIMENTAL SECTION

Materials and Methods. The synthesis of sodium **FS** has been described elsewhere.[22] The density of **FS**, which is required to estimate various parameters from X-ray diffraction data, was determined by taking a known mass of the dry powder in dichloromethane (a nonsolvent) into a 5 mL measuring cylinder and by measuring the increase in the dichloromethane volume. It was found to be 1.66 g/cm^3. All of the samples were prepared in deionized (miliQ) water and airtight screw cap vials. They were heated, vortexed several times, and visually inspected to be homogeneous before thermal equilibration, lasting from 3 h to 3 days. The vials were weighed before and after the heat treatment as well as after storage to ensure that there was no mass loss due to water evaporation.

A Nikon Eclipse E600 optical polarized microscope equipped with a Leica tilting compensator was used to observe the thermally equilibrated **FS**−water mixtures. ^{2}H NMR spectra were recorded on a Varian INOVA-300 spectrometer operating at 46.06 MHz with a typical spectral width of 100 kHz, acquisition time of 525 ms, and pulse width of 10 μs. Samples were prepared by weighing desired quantities of **FS** and D_2O directly in 5 mm NMR tubes, which were tightly closed and homogenized by several heating and vortexing cycles. The weights of the NMR tubes were verified before and after homogenization to monitor a possible loss of D_2O (typically below 0.001%). The samples were allowed to equilibrate at room temperature for at least 3 days. Measurements were done at 25 °C.

For SAXS, equilibrated **FS**−water mixtures in 0.7 mm flame-sealed capillaries were examined in a Bruker AXS D8 Discover X-ray diffractometer with a Hi-Star 2D detector using a Cu K_α source wavelength (1.54 Å). The incident beam was filtered by cross-coupled Göbel mirrors at 40 kV and 40 mA. The sample to detector distance was set at 30 cm. For freeze fracture electron microscopy (FF-TEM), a small sample drop was placed between two copper grids and inserted into gold planchettes. The "sandwich" was equilibrated in the controlled-environment vitrification system (CEVS) at 25 °C, vitrified in liquid ethane, and transferred into the BAF-060 replication system (BAL-TEC AG, Liechtenstein). In the BAF, the sandwich was opened, and the fractured surfaces were coated with platinum and carbon. The planchettes were thawed outside of the BAF, and the replicas were cleaned and then examined in a Tecnai 12 G^2 TEM at room temperature. Images were recorded on an Ultrascan 1000 2k × 2k sensitive CCD camera at nominal magnifications of up to 50k.[23]

3. RESULTS AND DISCUSSION

The aggregation behavior of **FS** at low concentration has been described elsewhere.[24] It is worth mentioning that **FS** is highly soluble in water at room temperature, and spherical micelles of around 3 nm diameter size start forming at 4 wt % **FS**.

The **FS**−water phase diagram was explored by first examining the optical texture of a range of samples by OPM. This was useful to identify lyotropic phases by their characteristic optical textures and determine the phase boundaries. Samples at [**FS**] below 63 wt % did not show birefringence, implying that they are composed of an isotropic

dx.doi.org/10.1021/jp311337z | J. Phys. Chem. B 2013, 117, 2820−2826

micellar phase (L_1). A mosaic texture with the presence of a few maltese crosses was observed at [**FS**] between 63 and 70 wt % (Phase I, Figure 2a). This optical texture is similar to the

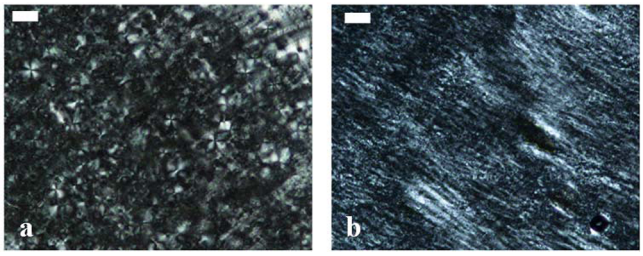

Figure 2. Representative OPM pictures of the lyotropic mesophases, at 25 °C. (a) 66 wt % **FS** (Phase I) and (b) 76 wt % **FS** (Phase II). The size of the scale bar is 50 μm.

pattern observed by Monduzzi and co-workers for a lyotropic phase with multilamellar vesicles.[10] The small features in the micrograph suggest that this LLC phase is composed of small domains. Above 70 wt % **FS**, a tightly packed streaky pattern, which is characteristic for the lamellar phase, was observed, (Phase II, Figure 2b).[10,25] Also, the viscosity of Phase II was higher compared to that of Phase I samples. Thus, two LLC phases were identified by OPM, Phase I between 63 and 70 wt % **FS** and and Phase II at [**FS**] between 70 and 84 wt %. Beyond 84 wt %, solid particles of surfactant and birefringent structures were observed (Figure S1, Supporting Information). Contact samples, in which a concentration gradient is present within the sample, were prepared by placing FS powder and a drop of water surrounding it between coverslip and glass slide. These samples have been investigated in order to check for additional mesophases. In particular, we were interested in bicontinuous mesophases, which exist in narrow concentration windows and are isotropic. None were found; therefore, we can be quite confident that only two LLC phases exist for the system.

^{2}H NMR measurements were performed to identify LLC phases and provide additional information regarding their structures. The shape of the ^{2}H NMR spectra is indicative of the alignment of water molecules embedded inside of the LLC phases, whereas the quadrupole splitting of the deuterium signal ($\Delta\nu_q$) from the D_2O in them quantifies the extent of the anisotropy present. In anisotropic liquid-crystalline samples, the deuterium signal splits into 2I lines (where I is the nuclear spin quantum number) separated by the splitting $\Delta\nu_q$, as given by eq 1.[26,27]

$$\Delta\nu_q = \frac{3}{4}C_q(3\cos^2\theta - 1) \quad (1)$$

In eq 1, θ is the angle between the external magnetic field and the averaged electric field gradient, which is parallel to the director of the phase, and C_q is the averaged quadrupole coupling constant, which is equal to $e^2qQ/\hbar$ (e is the absolute value of the electron charge, q is the electric field gradient, Q is the nuclear quadrupole moment, and $\hbar$ is the Planck constant). In isotropic liquids such as micellar solutions or bicontinuous cubic phases, θ changes very fast due to molecular motion. As a result, quadrupolar interactions are averaged to zero, and a single peak is observed.[28]

^{2}H NMR spectra of the **FS**–water mixture with [**FS**] between 60 and 80 wt % are shown in Figure 3.[29] At surfactant concentrations < 60 wt %, no splitting $\Delta\nu_q$ is observed, which

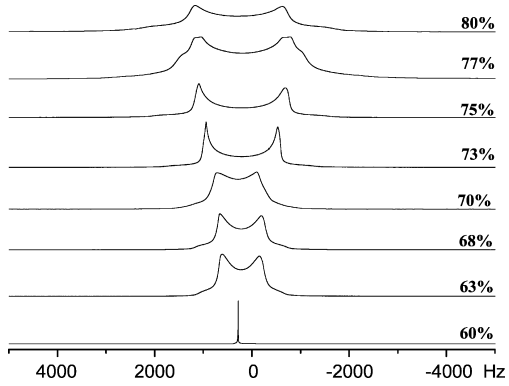

Figure 3. ^{2}H NMR spectra of aqueous **FS** samples at surfactant concentrations ranging from 60 to 80 wt % at 30 °C.

implies the presence of an isotropic, presumably micellar (L_1) phase (Figure 3). In contrast, at higher surfactant concentrations, a symmetric doublet with a quadrupolar splitting $\Delta\nu_q$ is observed, indicative of the presence of liquid-crystalline phases. The shape of the peaks is typical for a powder or "Pake" pattern,[7] and the line broadening can be ascribed to the presence of small-sized domains in Phase I,[30] which have been observed by optical microscopy and presence of nonaligned samples for the whole LLC regime.

In Figure 4, $\Delta\nu_q$ values are plotted against [**FS**] contents. Quadrupolar splitting values $\Delta\nu_q$ of Phase I samples remain

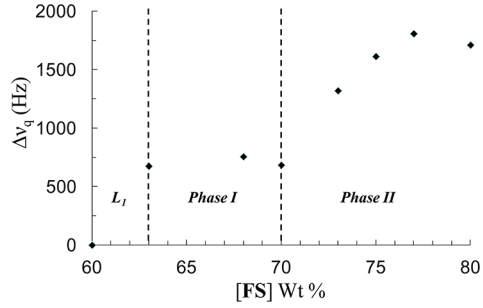

Figure 4. Quadruple splitting versus **FS** content (in wt%). The dotted line represents the C_S to L_α transition.

constant at around 700 Hz. Upon the formation of Phase II, $\Delta\nu_q$ values double (around 1300 Hz at [**FS**] 73 wt %) and increase linearly up to ~1800 Hz at [**FS**] 77 wt % and slightly decreases to ~1700 Hz at [**FS**] 80 wt %.[31]

Thus, ^{2}H NMR confirms that surfactant solutions are isotropic micellar below a concentration of 63% and form two anisotropic phases, Phase I and II from 63 to 70 wt % and from 70 to 80 wt %, respectively.

X-ray data provide geometrical parameters of the mesophases, originating from repeating layers composed of water and surfactant molecules. Diffraction patterns of aqueous **FS** mixtures measured by SAXS are shown in Figure 5. No significant diffraction peaks were observed below 60 wt %.

In Phase I, between 63 and 70 wt % **FS**, a single Bragg reflection was observed at **q** values between 0.44 and 0.48 Å^{-1}. The **q** value increases with [**FS**], which indicates a decrease of characteristic distances.

In Phase II, at [**FS**] larger than 70 wt %, a weak reflection at a **q** value of ~0.24 Å^{-1} started appearing along with the reflection at ~0.48 Å^{-1} that was already detected in Phase I. The Bragg

dx.doi.org/10.1021/jp311337z | J. Phys. Chem. B 2013, 117, 2820–2826

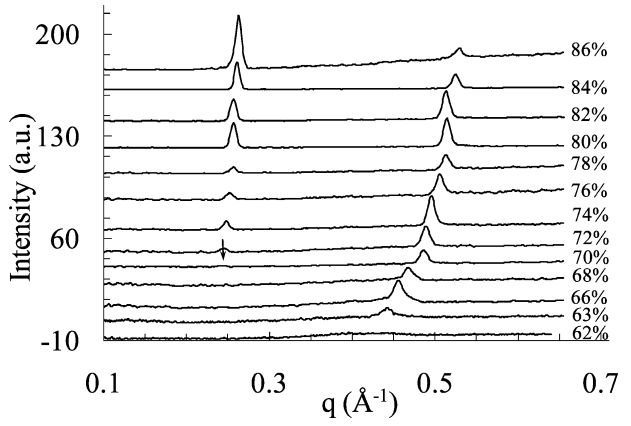

Figure 5. SAXS patterns for different aqueous **FS** solutions at 30 °C. The intensity is shown in arbitrary units. **q** is the wave vector. The arrow at 0.24 $Å^{-1}$ for the 70 wt % **FS** sample indicates the weak first-order reflection.

peak at 0.24 $Å^{-1}$ steadily shifted toward higher **q** values (from 0.24 to 0.26 $Å^{-1}$) with an increase in [**FS**]. Under all conditions, the high **q** value was exactly twice that of the low **q** value. Further, the intensity of the weak reflection at ∼0.24 $Å^{-1}$ steadily increased, whereas that of the ∼0.48 $Å^{-1}$ reflection decreased with an increase in [**FS**]. The intensity of both reflections became similar at 80 wt % [**FS**].

The change in the SAXS diffraction in Phase II, notable with the appearance of an additional reflection at 0.24 $Å^{-1}$, coincides with the change in the optical texture in OPM and a change in $\Delta\nu_q$ values from the ^{2}H NMR measurements.

The characteristic SAXS diffraction pattern with 1:1/2 reflections is indicative for the presence of a L_α phase between 70 and 84 wt % [**FS**]. The typical streaky OPM patterns and $\Delta\nu_q$ values that are higher than those from the samples in Phase I further support this assignment. The absence of Bragg reflections at lower **q**, in Phase I, and modulation in the relative intensities of both peaks in Phase II are attributed to the disappearing form factor at **q*** (any particular Bragg reflection, in this case, it is d_{001}) due to oriented bilayers.[32,33] Similar effects were observed in AOT−water lyotropic phases.[33]

LLC morphologies of **FS**−water mixtures were also investigated by freeze-fracture transmission electron microscopy (FF-TEM). This complementary technique is useful to obtain direct information on the 3D structure and the dimensions of the aggregates building up the LLC phases. The freeze-fracture image in Figure 6a reveals a complex morphology of rod-like structures, with diameters between 10 and 20 nm and lengths exceeding 100 nm (Phase I sample, 70 wt % **FS**). On a local scale, the rods are clearly oriented. A top view of these aggregates is shown in Figure 6b. The rod-like aggregates are clustered in stacks of 8−10 rods and organized into domains with hexagonal symmetry (Figure 6b, marked by arrows and hexagons). However, the domains are small, and long-range positional order among individual rods is absent.

Figure 6c shows a distinct morphology with flat layers in the Phase II sample at 77 wt % [**FS**]. The layered morphology clearly points to the presence of a lamellar L_α phase, which is in accordance with the data provided by the other techniques.

At this stage, it is clear that Phase II is a lamellar phase and that Phase I is a disordered columnar phase in which the columnar aggregates are heterogeneous in diameter and larger

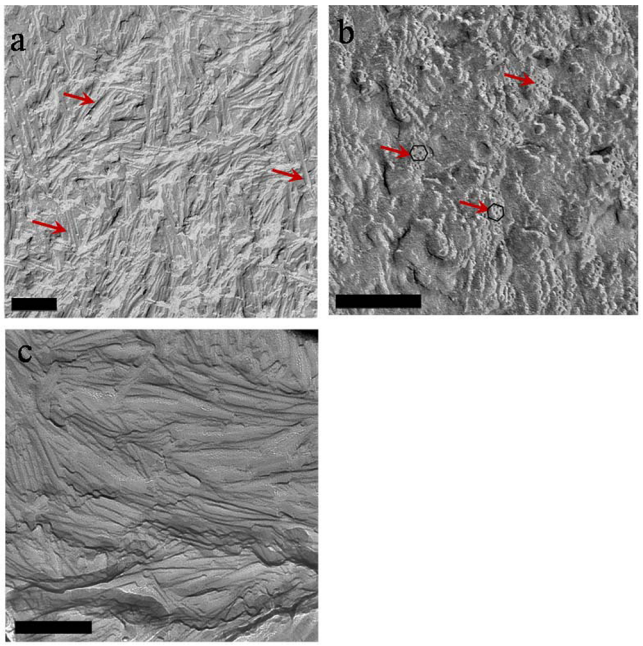

Figure 6. FF-TEM pictures of (a) a side view of rod-like aggregates and (b) their top view at 70 wt % **FS** contents; (c) the morphology of a lamellar LLC phase at 77 wt % **FS** contents. Scale bars = 200 nm. Arrows indicate the leek-shaped aggregates.

than the expected worm-like micelles. The lateral ordering of the columnar aggregates appears to be hexagonal.

Ultra low angle X-ray scattering did not reveal scattering originating from the lateral ordering of the columnar aggregates in the relevant size domain of 10−50 nm. This implies the absence of long-range order in the lateral direction. Presumably, the variations in the thickness of the rods,[34] which are observed in Figure 6a and b, prevents long-range positional ordering in the lateral direction. The lateral dimensions of the columnar aggregates indicate that probably they are multiwalled, leek-like aggregates. As these aggregates are heterogeneous in size, the number of surfactant layers must be different for the individual aggregates. The X-ray scattering that was observed for Phase I originates from the internal structure of the multiwalled aggregates and not from their positional ordering.

Here, it is noteworthy that the $\Delta\nu_q$ values obtained from ^{2}H NMR of Phase I samples are slightly less than half of those from Phase II (lamellar phase) samples, which suggests that the surrounding of the D_2O molecules has cylindrical geometry[7] in Phase I (see part B of the Appendix in the Supporting Information). Typically, such a change in $\Delta\nu_q$ values occurs during hexagonal to lamellar phase transitions. In our case, from SAXS and FF-TEM, it is clear that Phase I is not a hexagonal phase but a phase with leek-like supramolecular cylindrical aggregates, whereas Phase II is a lamellar (L_α) phase.

A detailed analysis of the surfactant layer thickness (L_S) and the water layer thickness (L_W) with increasing water fraction was conducted for Phase I and Phase II, based on the SAXS data, as described by eqs 2 and 3.[35,36] In eq 2, Φ_{FS} is the **FS** weight fraction, ρ_W and ρ_{FS} are water and **FS** densities, and d_{001} is the first-order reflection representing the bilayer thickness, respectively.

$$L_S = \frac{\Phi_{FS} d_{001} \rho_W}{\rho_{FS}(1 - \Phi_{FS}) + \rho_W \Phi_{FS}} \quad (2)$$

dx.doi.org/10.1021/jp311337z | J. Phys. Chem. B 2013, 117, 2820−2826

$$L_W = d_{001} - L_S \quad (3)$$

Similarly, the effective interfacial area per head group (A_{FS}) can be calculated using eq 4.

$$A_{FS} = \frac{2(V_{FS} + \alpha V_W)}{d_{001} N_A} \quad (4)$$

In eq 4, V_{FS} and V_W are molar volumes of the **FS** and water molecules, α is the molar ratio of water molecules to **FS** molecules, and N_A is Avogadro's number.

The results are compiled in Figures 7 and 8. Plots of d_{001}, L_S, and L_W (the primary Y axis) against α are shown in Figure 7. On the right Y axis, A_{FS} has been plotted against α.

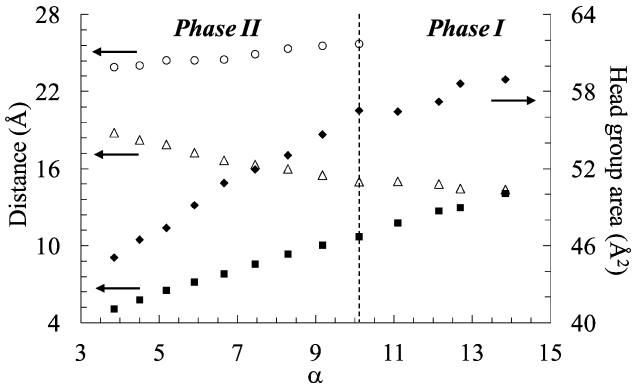

Figure 7. Plot of the first-order Bragg's reflection, d_{001} (○), hydrophobic layer thickness, L_S (Δ), water layer thickness, L_W (■), and area per head group of **FS**, A_{FS} (♦), normalized to the number of water molecules per surfactant molecule (α). The dotted line represents the boundary between the disordered columnar (C_S) and lamellar (L_α) phases. Values of L_S, L_W, and A_{FS} above α = 10 were calculated by assuming that the invisible first-order reflection (d_{001}) is exactly at half of the second-order reflection (d_{002}).

The value of d_{001} throughout the whole phase diagram ranges from 23.9 to 28.5 Å. These values are less than twice the length of an extended **FS** molecule (~30 Å), which is indicative of bilayer structures in both phases. In Phase II, d_{001} lies between 23.6 and 25.7 Å, and in Phase I, it is between 26.8 and 28.5 Å.[37]

The data in Figure 7 clearly show that the bilayer structure does not change significantly upon the transition from Phase I to Phase II. The values of L_S are lower than twice the length of the extended hydrophobic tails of **FS** (~22.5 Å), which suggests that the hydrophobic tails are partially interdigitated (Figure 8c), tilted (Figure 8b), or both (Figure 8d). Partial interdigitation of the surfactant tails is expected if we assume that the hydrocarbon and fluorocarbon phase separate, vide infra.

Throughout the phase diagram, L_S decreases (from 18.8 to 15.0 Å) with increasing α, whereas, L_W increases (from 5.1 to 14.0 Å). The effective interfacial area per head group, A_{FS} increases (from 45.1 to 59.0 Å^2) with α. A larger interdigitation and/or tilting of the hydrophobic chains was observed in Phase I than in Phase II. With an increase in the water concentration, a significant increase in A_{FS} is seen, unlike in nonionic surfactants.[11] This can be attributed to the increased electrostatic repulsion felt by the polar head groups of neighboring **FS** molecules with decreasing water concentration. The values of A_{FS} are closer to those reported for LLC phases of ammonium perfluorooctanoate.[35] The increase in d_{001} with α is not linear (Supporting Information and Figure S2). This suggests

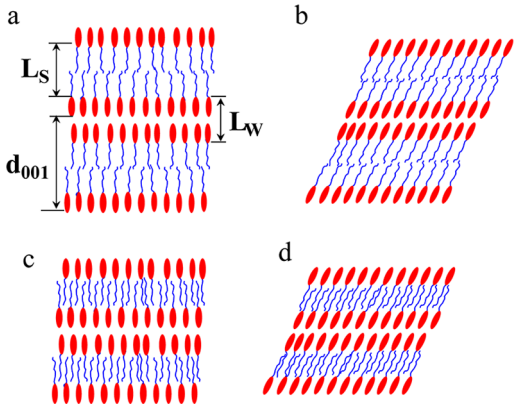

Figure 8. Possible arrangements for the surfactant bilayers. (a) Normal arrangement, (b) tilted bilayers, (c) interdigitated assembly of the surfactant molecules, and (d) tilted + interdigitated self-assembly. L_S represents the hydrophobic layer thickness, L_W the water layer thickness (including the **FS** head groups), and Id_{001} is the first-order Bragg reflection from the phase.

reorganization of the **FS** molecules with increasing water content.[38]

To the best of our knowledge, columnar lyotropic phases that are composed of multiwalled leek-like aggregates have not been previously reported. Interestingly, a hybrid phospholipid[19] has been reported to form micro- and nanotubules with leek-like arrangements of bilayers with a thickness of three bilayers. Interdigitation or tilting were observed within submicrometer-sized tubules that were formed in 3 wt % perfluoroalkylated glucophospholipid–water mixtures. Similar nanotubules have been observed in water solutions of a zwitterionic hybrid surfactant at 6 wt %.[20] These multilayer assemblies, however, are formed at low concentrations. Another hybrid surfactant, the star polyphile, reported by Hyde et al.,[14] displays a tilted hexagonal phase, in which the fluorocarbon and hydrocarbon chains are phase-separated within the hydrophobic domains.

On the basis of these observations, we postulate that phase separation within the hydrophobic domains of **FS** induces partial interdigitation and thereby reduces the layer thickness. The molecular structure of fully extended **FS**, which consists of an extensive and rigid fluorocarbon part and a slim hydrocarbon part, is depicted in Figure 9a. The lengths of the fluorocarbon and the hydrocarbon blocks are ~6.1 and ~5.0 Å, respectively, and the angle between them is ~20°. The fluorocarbon and the hydrocarbon blocks like to phase-separate, and the resulting interdigitated bilayer structure, with a thickness of ~24 Å, is

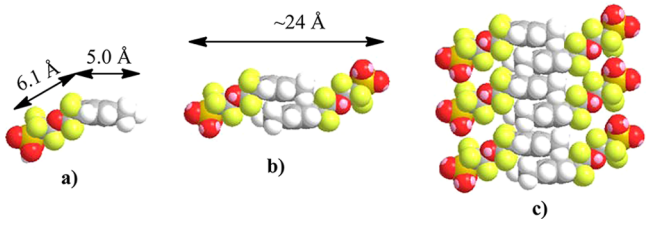

Figure 9. Molecular structures of (a) individual **FS** molecule, with arrows specifying the length of the hydrocarbon and fluorocarbon blocks. (b) Interdigitated arrangements of two **FS** molecules, with an estimate of the thickness of the entire bilayer, and (c) **FS** molecules in a bilayer.

dx.doi.org/10.1021/jp311337z | J. Phys. Chem. B 2013, 117, 2820–2826

presented in Figure 9b. The observed bilayer thickness, which includes the water layer, is around 28 Å at 63 wt % [**FS**].

Leek-like aggregates are formed by wrapping these bilayers around each other, as shown schematically in Figure 10.

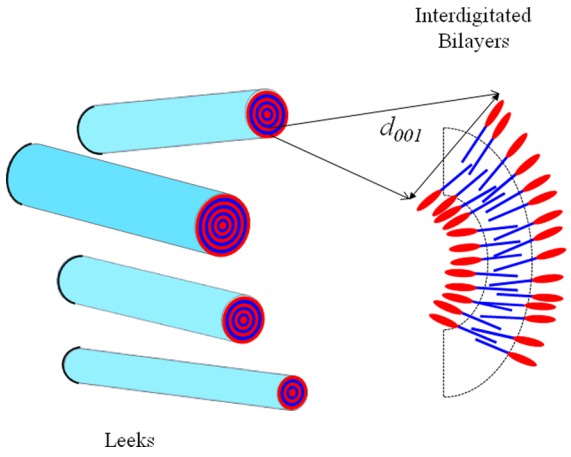

Figure 10. Schematic representation of the arrangement of **FS** molecules inside leeks with 2, 3, and 4 bilayers.

Assuming that the interior of the leeks is similar to worm-like micelles, which have diameters of 3 nm, and using an estimated bilayer thickness of ~28 Å, leeks with 2, 3, and 4 bilayers, with diameters of 14.2, 19.8, and 25.4 nm, respectively, may be present in Phase I.[39] Because the leeks are rigid and have decent persistence lengths, it is likely that the self-assembly of surfactant molecules into leek-like aggregates has induced the formation of the columnar phase. Clearly, the absence of any signal in ultra-low-angle X-ray suggests poor ordering of these leeks.

Thus, the supramolecular leeks self-organize into a disordered columnar phase (C_S), as seen in FF-TEM pictures (Figure 6b).

A schematic phase diagram for the **FS**–water binary system at 30 °C is shown in Figure 11. Above the critical micelle

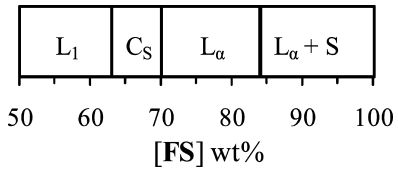

Figure 11. Schematic phase diagram of **FS**–water samples within the range of 25–30 °C. The marked phases are micellar (L_1), disordered columnar (C_S), lamellar (L_α), and lamellar + solid particles (L_α + S).

concentration, at around 4 wt %, the **FS**–water mixture displays an isotropic micellar phase (L_1) up to a concentration of 60–63 wt %. Between 63 and 70 wt % (Phase I), a disordered columnar C_S phase is formed, and from 70 up to 84 wt % (Phase II), a lamellar L_α phase was observed. Above this composition, a biphasic region with **FS** crystals along with the L_α phase was present. The C_S phase is characterized by a mosaic texture with maltese crosses in OPM and lower $\Delta\nu_q$ values than those in the L_α phase from ^{2}H NMR results. Additionally, it shows the presence of only a second-order reflection peak in a SAXS study and supramolecular leek-shaped aggregates in FFEM experiments.

The L_α phase is characterized by a tight streaky pattern in OPM and more than twice the $\Delta\nu_q$ values to those in the C_S phase. Also, it shows the characteristic 1:1/2 SAXS peak pattern and a distinct layered morphology in FF-TEM investigations

4. CONCLUSIONS

The LLC phase behavior of a fluorinated hybrid surfactant (**FS**) with water was investigated. Below 63 wt %, **FS** forms the isotropic micellar solutions. Between 63 and 84 wt % [**FS**], two phases are found. An unusual disordered columnar (C_S) phase composed of self-assembled leek-shaped aggregates has been observed in the concentration regime of 63 and 70 wt % [**FS**]. Those leeks were shown to be formed by wrapping up 3–5 **FS**–water bilayers around a worm-like micelle. Surprisingly, the **FS** molecules were arranged into partially interdigitated or tilted fashion and not organized in the "usual" tail-to-tail and head-to-head manner. A lamellar (L_α) phase was observed from 70 to 84 wt % [**FS**], with somewhat decreased interdigitation or tilting of the hydrophobic chains of the **FS** molecules. Above 84 wt %, a biphasic region with surfactant crystals dispersed in a lamellar phase was observed.

■ ASSOCIATED CONTENT

Ⓢ Supporting Information

Optical micrograph of the LLC phase sample at 88 wt % [**FS**], plot of −log of d_{001} against −log of the **FS** volume fraction. Table of d spacings for the first-order and second-order reflections with varying of the **FS** wt %. Appendix on the calculations of geometrical parameters from SAXS data and for calculations of maximum and minimum $\Delta\nu_q$ values for both LLC phases. This material is available free of charge via the Internet at http://pubs.acs.org.

■ AUTHOR INFORMATION

Corresponding Author

*E-mail: w.f.jager@tudelft.nl (W.F.J.); s.j.picken@tudelft.nl (S.J.P.).

Notes

The authors declare no competing financial interest.

■ ACKNOWLEDGMENTS

The authors thank the Ministry of Economic Affairs of The Netherlands for subsidizing this project via the EOS LT framework (EOS LT 02025). Partial support from the COST Action D43 is acknowledged. M.N.W. acknowledges Prof. Ernst J. R. Sudhölter for fruitful discussions and Mr. Ben Norder for helping in the SAXS experiments. M.N.W. is grateful for the assistance of Dr. K. Guruswamy and Mr. K. Sreenivas from NCL India in the ultra-low-angle X-ray study. D.D. thanks the financial support of the Israel Science Foundation and the Russell Berrie Nanotechnology Institute.

■ REFERENCES

(1) Israelachevili, J. N. *Intermolecular and Surface Forces*, 2nd ed.; Academic Press: New York, 1998; pp 390–391.
(2) Monduzzi, M. *Curr. Opin. Colloid Interface Sci.* **1998**, *3*, 467–477.
(3) Puntambekar, S.; Holmes, M. C.; Leaver, M. S. *Liq. Cryst.* **2000**, *27*, 743–747.
(4) Percec, V.; Glodde, M.; Johansson, G.; Balagurusamy, V. S. K.; Heiney, P. A. *Angew. Chem., Int. Ed.* **2003**, *42*, 4338–4342.
(5) González-Pérez, V.; Ruso, J. M.; Prieto, G.; Sarmiento, F. *J. Surfactants Deterg.* **2004**, *7*, 387–395.

(6) Kissa, E. *Fluorinated Surfactants and Repellents*; Marcel Dekker: New York, 2001; Chapters 1−2.
(7) Wang, K.; Orädd, G.; Almgren, M.; Asakawa, T.; Bergenståhl, B. *Langmuir* **2000**, *16*, 1042−1049.
(8) Fontell, K.; Lindman, B. *J. Phys. Chem.* **1983**, *87*, 3289−3297.
(9) Everiss, E.; Tiddy, G. J. T.; Wheeler, B. A. *J. Chem. Soc., Faraday Trans. 1* **1976**, *72*, 1747−1758.
(10) Mele, S.; Barry, W. N.; Monduzzi, M. *J. Phys. Chem. B* **2004**, *108*, 17751−17759.
(11) Ropers, M. H.; Stebe, M. *J. Phys. Chem. Chem. Phys.* **2001**, *3*, 4029−4036.
(12) Ropers, M. H.; Stebe, M. J.; Schmitt, V. *J. Phys. Chem. B* **1999**, *103*, 3468−3475.
(13) Sagisaka, M.; Fujita, Y.; Shimizu, Y.; Osanai, C.; Yoshizawa, A. *J. Colloid Interface Sci.* **2011**, *357*, 400−406.
(14) de Campo, L.; Varslot, T.; Moghaddam, M. J.; Kirkensgaard, J. J. K.; Mortensen, K.; Hyde, S. T. *Phys. Chem. Chem. Phys.* **2011**, *13*, 3139−3152.
(15) Regev, O.; Leaver, M. S.; Zhou, R.; Puntambekar, S. *Langmuir* **2001**, *17*, 5141−5149.
(16) Additional phases found between hexagonal and lamellar phases in two component surfactant−water systems have been termed as "intermediate" phases; see: Leigh, I. D.; McDonald, M. P.; Wood, R. M.; Tiddy, G. J. T.; Trevethan, M. A . *J. Chem. Soc., Faraday Trans. 1* **1981**, *77*, 2867−2876.
(17) Shinoda, K.; Hat, M.; Hayashi, T. *J. Phys. Chem. B* **1972**, *76*, 909−914.
(18) Tamori, K.; Esumi, K.; Meguro, K. *J. Colloid Interface Sci.* **1991**, *142*, 236−243.
(19) Imae, T.; Funayama, K.; Krafft, M. P.; Giulieri, F.; Tada, T.; Matsumoto, T. *J. Colloid Interface Sci.* **1999**, *212*, 330−337.
(20) Giulieri, F. G.; Krafft, M.- P.; Riess, J. G. *Angew. Chem., Int. Ed.* **1994**, *33*, 1514−1515.
(21) The LLC phases of this fluorinated glycolipid have not been reported on.
(22) Wadekar, M. N.; Jager, W. F.; Sudhölter, E. J. R.; Picken, S. J. *J. Org. Chem.* **2010**, *75*, 6814−6819 ; **FS** serves as a model fluorosurfactant that is similar in molecular structure to that of a polymerizable fluorinated surfactant (**PFS**). **PFS** can be polymerized to generate a membrane used for proton transportation in fuel cells. Therefore, by a two-step bottom-up approach, we first intend to investigate various mesophases of the **FS**−water system and then exploit the know-how obtained from the phase behavior and morphologies of it to create self-assembled nanostructured membranes by polymerizing the desired mesophases of the **PFS**−water system..
(23) Danino, D.; Bernheim-Groswasser, A.; Talmon, Y. *Colloids Surf., A* **2001**, *183*, 113−122.
(24) Wadekar, M. N.; Boekhoven, J.; Jager, W. F.; Koper, G. J. M.; Picken, S. J. *Langmuir* **2012**, *28*, 3397−3402.
(25) Kunieda, H.; Shigeta, K.; Ozaw, K. *J. Phys. Chem. B* **1997**, *101*, 7952−7957.
(26) Blackburn, J. C.; Kilpatrick, P. K. *J. Colloid Interface Sci.* **1992**, *149*, 450−471.
(27) Ghosh, S. K.; Rathee, V.; Krishnaswamy, R.; Raghunathan, V. A.; Sood, A. K. *Langmuir* **2009**, *25*, 8497−8506.
(28) Sjöbom, M. B.; Edlund, H.; Lindström, B. *Langmuir* **1999**, *15*, 2654−2660.
(29) It was difficult to prepare homogeneous samples inside of NMR tubes above 80 wt %.
(30) Smith, A. M.; Holmes, M. C.; Pitt, A.; Harrison, W.; Tiddy, G. J. T. *Langmuir* **1995**, *11*, 4202−4204.
(31) Usually, $\Delta\nu_q$ values gradually increase with an increase in surfactant concentration through the anisotropic−anisotropic LLC phase transition, within the whole phase diagram
(32) Ropers, M. -H.; Stèbè, M. −J.; Schmitt, V. *J. Phys. Chem. B* **1999**, *103*, 3468−3475.
(33) Nallet, F.; Laversanne, R.; Roux, D. *J. Phys. II* **1993**, *3*, 487−502.
(34) The stimated rod thickness from Figure 6a is ∼10 nm, whereas from Figure 6b, it is around 20−30 nm thick.
(35) Luzzati, V.; Mustacchi, H.; Skoulios, A.; Husson, F. *Acta Crystallogr.* **1960**, *13*, 660−667.
(36) Ropers, M.- H.; Stebe, M.- J. *Phys. Chem. Chem. Phys.* **2001**, *3*, 4029−4036.
(37) L_S and L_W for $\alpha > 10$ (Phase I) were calculated assuming that the position of the undetected first-order Bragg peak was located at twice the **q** value of the observed second-order reflection.
(38) Fontell, K. *J. Colloid Interface Sci.* **1973**, *44*, 318−329.
(39) Splitting of the leek-like aggregates has not been observed in the FFEM images, and therefore, a direct count of the number of bilayers in one leek-shaped aggregate could not be made.